International Scholars Journals

International Journal of Urology and Nephrology ISSN 2091-1254 Vol. 8 (2), pp. 001-009, February, 2020. Available online at www.internationalscholarsjournals.org © International Scholars Journals

Full Length Research Paper

Differential analysis of human kidney stone samples using electrospray ionization mass spectrometry

Zhiquan Zhou[1], Yongzhong Ouyang[2], Xiangtai Zeng[3], Tingting Zhang[1], Bin Jia[2], Xinglei Zhang[2], Huanwen Chen[2] and Jianhua Ding [2]*

[1]Institute of Information Engineering, Harbin Institute of Technology, Weihai, 264209, P. R. China. [2]Jiangxi Key Laboratory for Mass Spectrometry and Instrumentation, Biology and Material Science, College of Chemistry, East China Institute of Technology, Nanchang, 330013, P. R. China. [3]Department of Surgery, 2nd Hospital of Gannan Medical University, Xinfeng, 341600, P. R. China.

Accepted 21 October, 2019

Kidney stones may be caused by many factors, including ingestion of melamine for a relatively long time. The diagnosis of melamine-induced kidney stones and the understanding of how the melamine is involved in the formation of kidney stones are of practical importance. To establish a sensitive method based on widely used electrospray ionization mass spectrometry (ESI-MS) for diagnosis of melamine-induced kidney stones and to probe the differential formation of melamine-induced kidney stones at molecular levels. Human kidney stones were collected in hospital from 6 groups of patients at different ages. ESI-MS was employed as the main technique with the principal component analysis for data processing. Using principal component analysis (PCA) of the ESI-MS fingerprints, a set of 21 melamine-induced kidney stone samples and 21 uric acid derived kidney stone samples were successfully differentiated from the other groups, rendering ESI-MS method a potential platform for differential analysis of the human kidney stones of various causes at molecular levels. The experimental results also indicate that in addition to the melamine, the chemical compounds enwrapped in the melamine-induced kidney stone samples are different from other kidney stone samples. These findings suggest that ESI-MS is a useful tool for diagnosis of melamine-induced kidney stone samples and the melamine-induced kidney stone could be formed by different mechanisms.

Key words: Toxicity of melamine, chemical profiling, uric acid, electrospray ionization-mass spectrometry (ESI-MS), kidney stone, melamine, principal component analysis.

INTRODUCTION

Kidney stones, one of the most painful urologic disorders, have beset humans for centuries. It is estimated that about three percent of the world's population will suffer from kidney stones in their lifetime (Johnson et al., 1979; Coe et al., 1996). Annually, about 3 million people need medical care due to kidney stone problems (Coe et al., 1996; Hiatt et al., 1996). Kidney stones in human are normally caused by many factors, such as the diet and genetics (Anderson, 2002). For example, it is known that the ingestion of melamine illicitly used in food may cause the formation of kidney stones in both humans (Lam et al., 2009) and animals (Baynes et al., 2008). Although, the formation mechanism for the melamine-induced kidney stones remains unclear, unambiguous chemical profiling of the melamine-induced human kidney stones is urgently required for better medical care performance. Chinese government covers all the medical expenditures for the melamine-induced kidney stone diseases after the melamine event, while patients suffering from uric acid-induced kidney stones are not included (Chan and Lai, 2009). Thus, accurate detection of melamine-induced human kidney stones and the study of the formation mechanism as well are of great significance to both clinics

*Corresponding author. E-mail: Dingjianh2004@126.com. Tel: 0086-791-3896370. Fax: 0086-791-3896370.

Table 1. Clinical data of human kidney stone samples.

Patient number	Age	Sex	Quantity and period	Stone location	Imaging studies
Sample 1	26 month	Male	30 - 50 g/day, 2 years	Left ureter	Nonopaque stone
Sample 2	36 month	Female	30 - 50 g/day, 1.5 years	Left kidney pelvis	Nonopaque stone
Sample 3	7 years	Male	30 - 50 g/day, 2.5 years	Left kidney pelvis	Radiopaque
Sample 4	17 month	Male	30 - 50 g/day, 1.5 year	Left kidney pelvis	Radiopaque
Sample 5	48 years	Female	No drinking	Right ureter	Radiopaque
Sample 6	44 years	Male	No drinking	Left kidney pelvis	Radiopaque

diagnosis and economic interests.

X-ray inspection provides valuable information about the size and location of the kidney stone, and thus, it is the most common technique for clinical diagnosis of the calcium oxalate stones (Herring, 1962; Pietrow and Karellas, 2006). However, about 10% of radiolucent kidney stones, such as melamine-induced stone, do not contain enough calcium to be detected by standard X-ray imaging methods. Currently, computed tomography (CT) is considered as the gold standard diagnostic test for the detection of kidney stones (Ferrandino et al., 2010; Otnes,1983), and most of them are detectable by CT except for very rare stones, which are composed of drug residues in the urine (Pietrow and Karellas, 2006). However, the CT scans impose a radiation exposure and a high cost on patients, and thus, it is not the best choice for clinical diagnosis. Ultrasound imaging is alternatively useful for the detection of kidney stones as it gives details about the presence of hydronephrosis, particularly, for cases where X-ray/CT imaging is discouraged (Jia et al., 2009; Sun et al., 2009). However, the results of ultrasound imaging are highly dependent on the clinical observations and statistics (Wen et al., 2009; Zhang et al., 2009). Infrared spectroscopy and Raman spectroscopy detects limited categories of urinary stones (Chiu et al., 2010; Evan et al., 2005). The chemical elements in the stones, such as calcium, phosphorus, oxygen, carbon, etc., can be detected using scanning electron microscopy (SEM) combined with Fourier transform infrared spectroscopy (FTIR) (Marickar et al., 2009). However, the presence of melamine in the stone samples can not be determined. So far, there is no reliable method available for fast differentiation of the melamine-induced kidney stone from other types.

Recently, surface desorption atmospheric pressure chemical ionization (SDAPCI) (Yang et al., 2009a, b, c; Chen et al., 2007) has been successfully employed for direct analysis of melamine tainted powdered milk samples, with minimal sample pretreatment. This provides the potential feasibility for detection of melamine in kidney stone samples by SDAPCI-MS, which will be described in other studies. Methods based on electrospray ionization mass spectrometry (ESI-MS) have been widely used for rapid differentiation of quality of volatile liquid foods (De Souza et al., 2007; Mendonça et al., 2008; Sanvido et al., 2010; Biasotoa et al., 2010; Alves et al., 2010). In this study, an electrospray mass spectrometric method has been applied for the chemical profiling of kidney stone solution samples. Melamine-induced kidney stones and uric acid derived kidney stones have been differentiated by performing principal component analysis (PCA) with the mass spectral raw data, which were recorded under either positive or negative ion detection mode. Since neither time consuming steps for separation of the sample nor expensive MS^n instrument for molecular structure identification is required for differentiation of the melamine-induced kidney stone samples, the results suggest that the ESI-MS-based method reported here can be particularly useful for rapid differentiation of kidney stones at the molecular level.

METHODOLOGY

Materials and sample preparation

The human kidney stone samples for 6 patients were provided by the Hospital of Gannan Medical University. As shown in Table 1, the patients for sample 1 to 4 are little children (not more than 7 years old) who are possible victims of melamine tainted milk event (Xin and Stone, 2008) that happened in China. There is no clear evidence showing that the powder milks consumed by these patients were contaminated with melamine. As recorded in the clinical data sheet, patient 3, a 7 year old boy, had consumed powdered milk for the longest time. The preliminary work performed in a Canada lab using secondary ion mass spectrometry (Sodhi et al., 2010) also shows that melamine indeed exists in the calculus from the patient 3. Patients 5 and 6 are adults, who did not consume any milk products. Therefore, the stone samples from patients 5 and 6 were used as the reference samples. The kidney stone samples (1 to 5 mg) were dissolved in 10 ml acetic acid/methanol solution (1:4, v/v) and ultrasonicated for 20 min (10 W power) to assist dissolution. The solution was then diluted 1000 times with methanol/water (1:1, v/v) solvent for the ESI-MS analysis. Chemicals, such as methanol (analytical reagent (AR) grade) and acetic acid (AR grade) were bought from Chinese Chemical Reagent Co. Ltd. (Shanghai, China).

ESI-LTQ mass spectrometer

The experiments were carried out using a commercial available linear ion trap mass spectrometer (LTQ-XL, Finnigan, San Jose, CA)

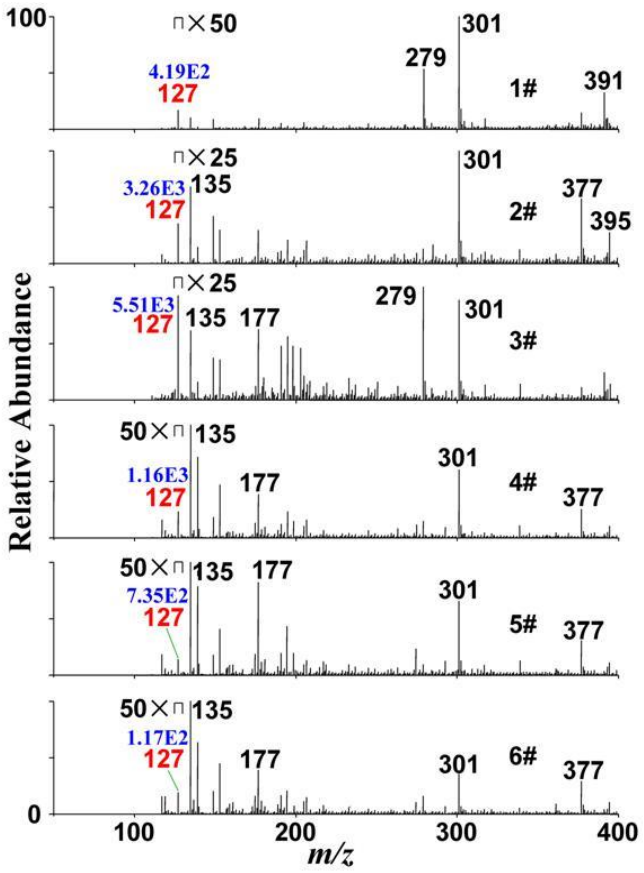

Figure 1. Mass spectrum recorded using positive ESI-MS from different kidney stone solution samples. 1 to 6#: the stone from patient 1 to 6, respectively.

installed with an ESI source. The ESI source and the LTQ mass spectrometer were set to work under positive/negative ion detection mode. The nebulizing gas (N_2) pressure was 1 MPa, the ESI high voltage was +4.5 kV/-3.5kV, and the temperature of the ion introduction capillary was 350°C. Other parameters were set at default values of the instrument and no further optimization of the ESI-MS was performed.

Data acquisition and analysis

The full scan mass spectra were recorded for an average acquisition time of 30 s. Collision induced dissociation (CID) was performed with 20 to 37% collision energy (CE). The parent ions were isolated with a mass window width of 1.5 Da, and the mass spectrometry/mass spectrometry (MS/MS) spectra were collected for a recording time of more than 30 s if necessary. Principal component analysis (PCA) of the mass spectral fingerprint data was performed in Matlab (version 7.0, Mathworks Inc., Natick, U.S.A.). The mass spectral data were exported to Microsoft Excel and the data were arranged using the mass to charge (*m/z)* values as independent variables and using the relative abundance of the full scan mass fingerprint (MS^1) as the dependent variables. The whole mass spectra data were treated as a matrix X, in which the rows and the columns corresponded to sample cases and *m/z* value variables, respectively. All the mass spectral data expressed by the relative abundance were directly used for the PCA. The '*princomp*' function included in the '*Matlab Toolbox*' was used for the PCA processing. When the PCA was completed, the scores of the first three principal components (PCs) were exported to new spreadsheets, and then Matlab was used to present the results of statistical analysis for better visualization.

RESULTS AND DISCUSSION

ESI-MS analysis

Generally, different types of kidney stones vary in chemical compositions, but most of the kidney stones are composed of calcium oxalate, calcium phosphate and magnesium ammonium phosphate (Moe, 2006; Millman et al., 1982). Dissolved in acetic acid/methanol solution, the corresponding metal salts, such as calcium acetic, magnesium acetic, etc., were formed. ESI-MS provides information-rich spectra and many species can be simultaneously detected. Note that the solid kidney stones must be dissolved into liquid form prior to ESI-MS measurements. In order to avoid the contamination of the ESI-MS instrument, the stone solutions were diluted 1000 times with methanol/water (1:1, v/v) solvent before they were electrosprayed for further MS analysis.

The mass spectra of the six samples were recorded under the positive ion detection mode. As shown in Figure 1, a set of peaks, such as *m/z* 127, 135, 177, 279, 301 and 377 appeared in all the six samples. It was known that the peaks at *m/z* 279 and 301 were the protonated dibutyl phthalate (DBP) (Hu et al., 2010) and $[DBP+Na]^+$, respectively, due to the DBP used as plasticizers in the instrument system. Although, the signal of *m/z* 127 was recorded in all the six samples, the intensity of *m/z* 127 detected in the sample from patients 1, 5 and 6 was in an order of magnitude less than those detected from the others. Furthermore, in the CID experiments, the precursor ions at *m/z* 127 detected from the sample 3 generated ions of *m/z* 43 ($CH_3N_2^+$), 85 ($C_2H_5N_4^+$) and 110 ($C_3H_4N_5^+$) as the major fragments (Figure 2a) by the loss of $C_2H_4N_4$, CH_2N_2 and NH_3, respectively. In the MS^3 experiment, a characteristic fragment of *m/z* 43 ($CH_3N_2^+$) was successively produced from the fragmentation of *m/z* 85 (Figure 2b) or 110 (Figure 2c). These fragmentation patterns match with those obtained with authentic melamine samples and are in accordance with the fragmentation pathways of protonated melamine observed in previous studies (Zhu et al., 2009). Consequently, the peak at *m/z* 127 detected from sample 3 was confirmed to the protonated melamine molecule $(M+H)^+$. However, these characteristic fragments could not be produced from the other stones (samples 1, 2, 4, 5 and 6) (Figure 3), indicating that only sample 3 is the melamine-induced kidney stone among these stones.

Upon negative ion detection mode, calcium and magnesium acetate salts formed the corresponding deprotonated ions, such as $(CaAC_2)AC^-$ (*m/z* 217),

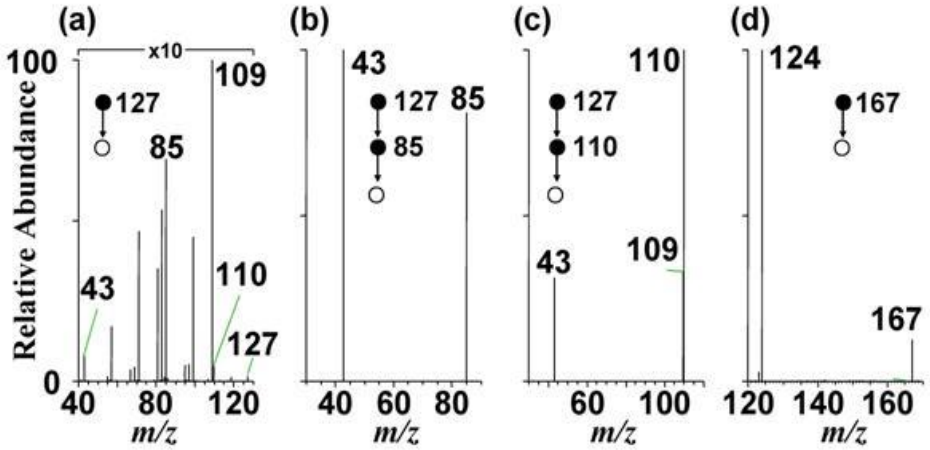

Figure 2. Mass spectra recorded by ESI-MS. (a) MS/MS spectrum of protonated melamine (*m/z* 127) in sample 3; (b) MS/MS/MS spectrum of the ionic fragments (*m/z* 85) produced from protonated melamine (*m/z* 127) in sample 3; (c) MS/MS/MS spectrum of the ionic fragments (*m/z* 110) produced from protonated melamine (*m/z* 127) in sample 3; (d) MS/MS spectrum of deprotonated uric acid (*m/z* 167) in sample 2.

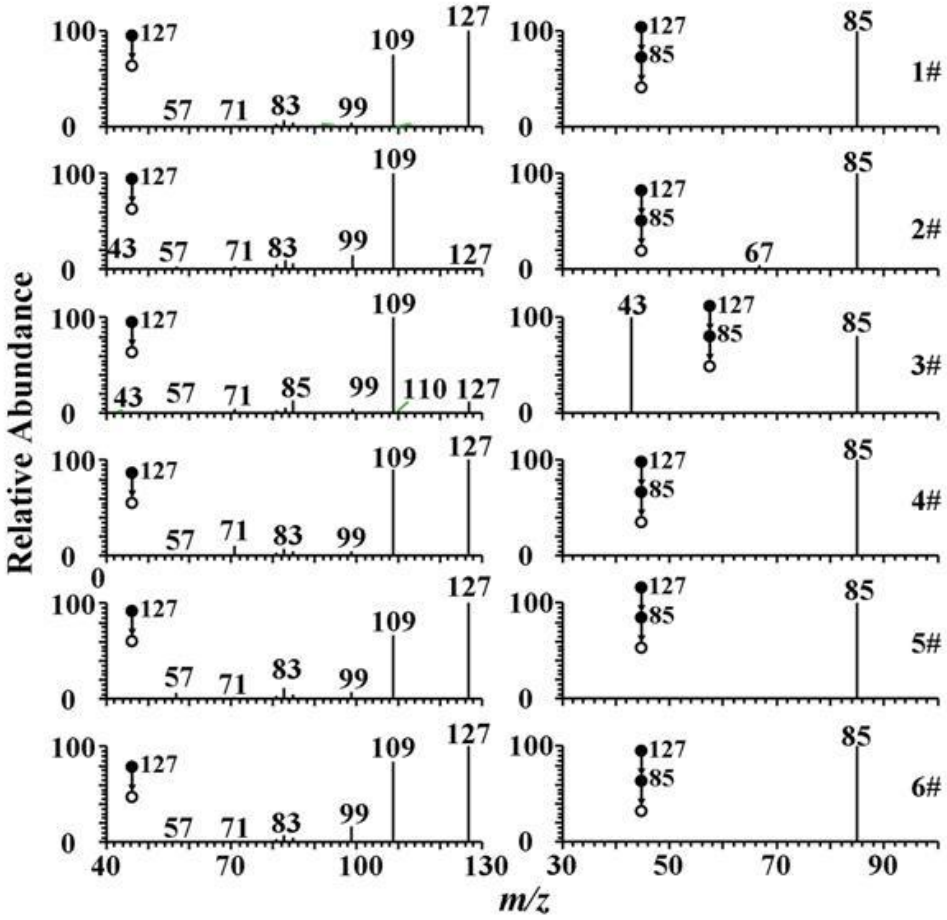

Figure 3. MS/MS spectra of precursor ions (*m/z* 127) and MS/MS/MS spectra of ionic fragments (*m/z* 85) produced from *m/z* 127 from different kidney stone solution samples. 1 to 6#: the stone from patient 1 to 6, respectively.

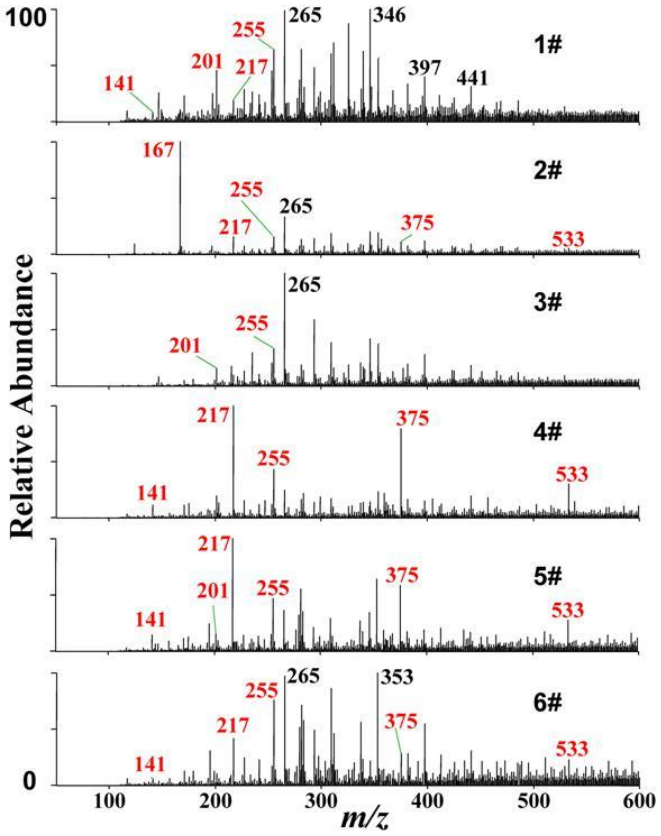

Figure 4. Upon the negative ion detection mode, ESI mass spectrum recorded from the kidney stone solution samples. 1 to 6#: the stone from patient 1 to 6, respectively.

$(CaAC_2)_2AC^-$ (*m/z* 375), $(CaAC_2)_3AC^-$ (*m/z* 533), $(MgAC_2)AC^-$ (*m/z* 201), $(NaAC)AC^-$ (*m/z* 141) and $(KAC)_2AC^-$ (*m/z* 255), as shown in the Figure 4. It is noteworthy that significant abundant peaks at *m/z* 167 is present only in sample 2, while other MS peaks for sample 2 are much lower than those in other samples, suggesting that sample 2 might have different chemical contents. Upon CID, the precursor ions of *m/z* 167 generated the abundant fragments of *m/z* 124 ($C_4H_2N_3O_2^-$) by the loss of CHNO (Figure 2d). These characteristic fragments were in good agreement with previous work of uric acid (Dai et al., 2007). Furthermore, CID data also matched with those recorded using authentic uric acid compound under the same experimental conditions. Therefore, the ions at *m/z* 167 in the samples were assigned to be the deprotonated uric acid. In comparison with other samples, abundance of *m/z* 167 in sample 2 suggests that the content of uric acid in kidney stone samples 2 should be much higher than others. Accordingly, the cause of the kidney stone for baby girl (patient 2) could be diagnosed as uric acid.

In a related study, the same groups of samples were investigated using time-of-flight secondary ion mass spectrometry (ToF-SIMS) (Sodhi et al., 2010). Polished cross-sections of the samples were obtained for recording SIMS mass spectra in both high spatial and high mass resolution modes. The motivation was to distinguish between different stone types using the distribution patterns of the N-containing species obtained in the ToF-SIMS experimental data. Although, some interesting data were obtained, the SIMS technique was not able to detect melamine molecules from the melamine-induced stone sample. The results obtained using ESI-MS in this work differentiated melamine-induced kidney stones from the uric acid-based kidney stones, showing that ESI-MS provides complementary information for the ToF-SIMS results. The combination of these two techniques is promising for the understanding of the formation mechanism of the kidney stones. For the clinic diagnosis purpose, however, ESI-MS is of obvious advantages, including simple operation, low cost instrument and fast analysis speed, especially when PCA is applied to process the experimental data (demonstrated subsequently).

Principal component analysis (PCA)

As mentioned earlier, the melamine and uric acid induced human kidney stones can be differentiated under the positive and/or negative mode of ESI-MS/MS experiments. However, the sensitive CID measurements require an instrument of advanced tandem MS capability. This requirement demands expensive mass spectrometers. As shown in the full scan mass spectra, more signals rather than the melamine itself (*m/z* 127) were differentiable in the mass spectral fingerprints. Once the differences are clearly visualized, the melamine-induced kidney stones can be reliably diagnosed without resorting to tandem MS experiments, featured on site applications, using simple and low cost portable mass spectrometers. Therefore, PCA, a powerful tool for data compression and information extraction (Jackson, 1980; Moore, 1981; Tipping and Bishop, 1999) was employed to process the ESI-MS data for differentiation of the samples.

As a result, a PCA score plot of six types of stone samples are shown in Figure 5, among which a1 and a2 correspond to the data points of full ESI mass spectrum recorded upon the positive ion detection mode. Note that, there are 21 data points generated for the groups of all six patients, using 21 pieces of the stone samples from the same patient. As shown in Figure 5a1 and a2, a total of 126 data points were explained by the score graphs of PC1-PC2 and PC2-PC3. 91.9% of the total variations were represented and the percentages of variance exp-lained by PC1, PC2 and PC3 were 54.73, 25.20 and 11.97%, respectively. Except for samples 4 and 6 which can not be distinguished from each other, others were all differentia-ted from each other. The differentiation of samples 1, 2

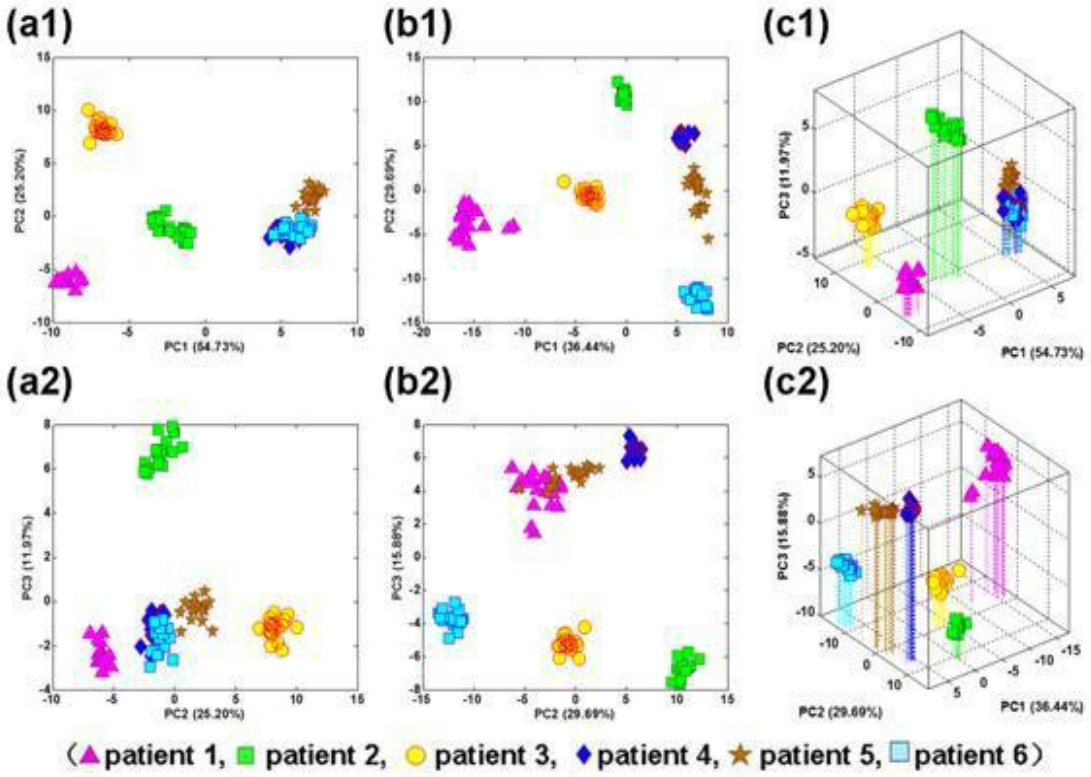

Figure 5. PCA score results for differentiation of the human kidney stones. a1: score plot PC1-PC2 based on positive ESI; a2: score plot PC2-PC3 based on positive ESI; b1: score plot PC1-PC2 under negative ESI ion mode; b2: score plot PC2-PC3 under negative ESI ion mode. c1: 3D-score plot PC1-PC2 under positive ESI c2: 3-D score plot under negative ESI.

(uric acid induced stones) and 3 (melamine-induced stones) has been achieved. On the other hand, the distribution of signs in each cluster from samples 4 to 6 is restricted in a narrow scope. Thus, the PCs show strong ability for differentiation of melamine and uric acid induced stones from the other types of kidney stones. Although, a few data points of sample 5 were mixed together with samples 4 and 6 in the PC1 and PC2 plane (Figure 5a1), all the data points of sample 5 were completely separated from the other samples in PC3, as shown in Figure 5a2. However, upon the negative ion detection mode, the six different types of kidney stones were differentiated from each other in the PC1 and PC2 plane (Figure 5b1), and this could be clearly visualized in the corresponding 3-D space (Figure 5c2). Therefore, negative ESI-MS is proposed for differentiation of the kidney stone samples without CID experiments, although the melamine induced stones have been differentiated from the others under the positive ion mode.

As shown in the clinical data (Table 1), the different X-ray imaging properties (both the stone location and transparency) of sample 1 from sample 5 might explain the separation of samples 1 and 5 in the PCA score plots. In both Figure 5b1 and 5b2, 1.5-year history of powdered milk intake was most likely to be the only factor for differentiating sample 4 from sample 6 in the PCA score plots, since the stones in patients 4 and 6 were both located in the left kidney pelvis and were all radiopaque in the X-ray imaging studied in the clinical examination. Although, the stones in patient 5 were also radiopaque, the location of the stone 5 was at the right ureter instead of the left kidney pelvis. This could be the important factor for differentiating sample 5 from either sample 4 or sample 6. Similar to sample 5, the stone in sample 1 was also located in the ureter (the left ureter), but it was radiolucent in the X-ray imaging study, indicating that the chemical composition of sample 1 should be different from the opaque samples. In the PCA score plots, sample 2 was located remarkably far from the sample 3, because sample 2 was uric acid induced kidney stones, which should be chemically different from the melamine induced kidney stones. Conclusively, the location and imaging property of kidney stones are two of the most important factors used to distinguish these kidney stones and they play important roles in differentiating different types of kidney stones after performing PCA.

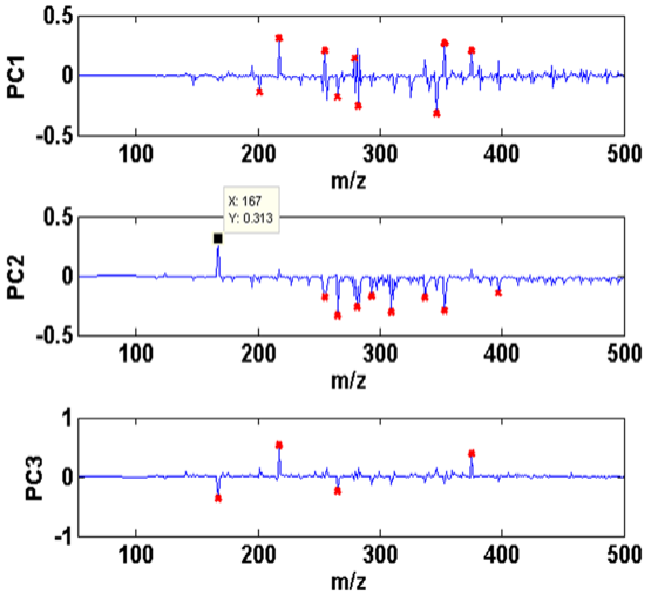

Figure 6. PCA loading results for the PCs based on the negative ESI.

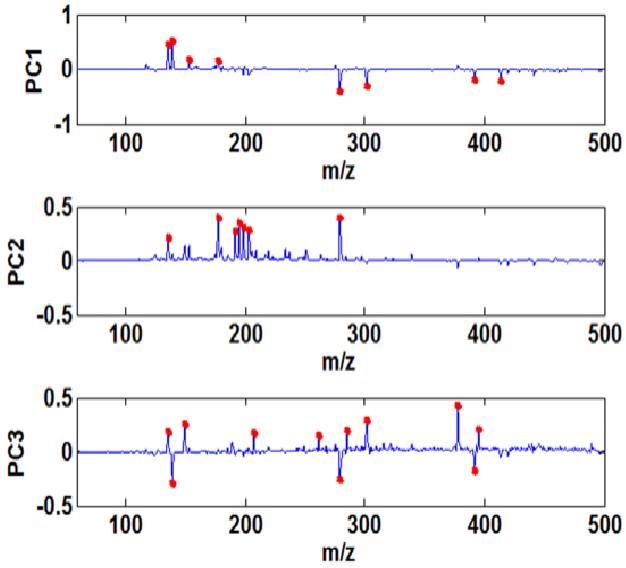

Figure 7. PCA loading results for the PCs based on the positive ESI.

Figure 6 presents the PCA loading plots of the 126 data points upon negative ion detection. The major differential peaks (that is, peaks of significant abundances in the PCA loading plots, which correspond to the ions that contributed most to differentiation of the samples) shown in the PCA loading plots, could potentially be useful as molecular markers for differentiating different kidney stones. For example, the most predominant ions in the loading of PC2, which corresponded to the deprotonated uric acid (*m/z* 167), could serve as the most important factor for differentiating the uric acid induced kidney stone (patient 2) from the others. For this reason, typical differential peaks at *m/z* 167, 255, 265, 279, 281, 282, 311, 337, 346, 353, 375 and 397 were selected as molecular markers, because they were outstanding in the PCA loading plots. Structural identification of all these differential peaks is theoretically possible using tandem mass spectrometry experiments, but it is beyond the scope of this study. Also, Figure 7 gives the loading plots of 126 data points under positive ion detection model. It is clear that the peaks at *m/z* 135, 139, 149, 177, 191, 195, 198, 203, 207, 261, 285, 301, 377, 391 and 413 contributed most to differentiation of these samples, and could be regarded as molecular markers for differentiating different kidney stones. The absence of the ion at *m/z* 127 in the load plots suggests that the ion at *m/z* 127 is not the important variable in the differentiation of these samples in the full ESI scan mass spectra, although the confirmation of melamine-contained sample requires the MS/MS of the ion at 127 and MS^3 of the ionic fragments at *m/z* 85 produced from the *m/z* 127. This is because, the ion at *m/z* 127 can be observed in all the six samples in the full ESI scan experiments, due to disturbance of impurities.

In summary, the full mass spectra could be collected in a few seconds using ESI mass spectrometry with minimal sample pretreatment, indicating that ESI-MS affords high analysis speed. Sufficient information used for differentiation of different kidney stones could be provided, even though the stone liquid solutions were diluted 1000 times before introducing into the ESI ionization, demonstrating high sensitivity of the ESI-MS. Good results for differentiation of melamine and uric acid induced kidney stones from the others whenever the positive or negative ion mode was used, to a certain degree, and they showed the stability and reproducibility of the ESI. Therefore, ESI-MS-based method proposed in this study is indeed a practical technique for rapid differentiation of kidney stones, with its high analysis speed, high sensitivity and good reproducibility.

Conclusions

An ESI-MS-based method was applied for fast detection of the melamine-induced and uric acid derived human kidney stone samples with minimal sample pretreatment. Using the tandem mass spectrometry, specific compounds, such as melamine and uric acid have been identified with high confidence. On the other hand, without the need of tandem MS capability, the ESI-MS combined with PCA is an analytical tool for differentiation of different types of human kidney stones, and is especially useful for

the negative ESI-MS mass spectral fingerprints in the analysis and detection of melamine-induced kidney stones. Melamine, a basic compound, could not be detected in the negative ESI mass spectra. However, it has been experimentally demonstrated that many other chemicals detected from the melamine-induced kidney stone samples were different from those detected from other types of kidney stone samples. These findings are the sound bases at molecular level for differentiation of the melamine-induced kidney stones from the others, particularly in the negative ion detection mode, and they provide useful hints for further study on the formation mechanisms of melamine-induced kidney stones in the pathological research.

ACKNOWLEDGEMENT

This work was jointly supported by the National Instrumentation Program (No. 2011YQ170067) and the Major Grant of Natural Science Foundation of Jiangxi Province (No. 2010GZH002).

REFERENCES

Alves JdO, Neto WB, Mitsutake H, Alves PSP, Augusti R (2010). Extra virgin (EV) and ordinary (ON) olive oils: Distinction and detection of adulteration (EV with ON) as determined by direct infusion electrospray ionization mass spectrometry and chemometric approaches. Rapid Commun. Mass Spectrom., 24: 1875-1880.

Anderson RA (2002). A complementary approach to urolithiasis prevention. World J. Urol., 20: 294-301.

Baynes RE, Smith G, Mason SE, Barrett E, Barlow BM, Riviere JE (2008). Pharmacokinetics of melamine in pigs following intravenous administration. Food. Chem. Toxicol., 46: 1196-1200.

Biasotoa ACT, Catharinob RR, Sanvidoc GB, Eberlinc MN, da Silvaa MAAP (2010). Flavour characterization of red wines by descriptive analysis and ESI mass spectrometry. Food Qua. Preference, 21: 755-762.

Chan ZCY, Lai WF (2009). Revisiting the melamine contamination event in China: Implications for ethics in food technology. Trends. Food. Scl. Tech., 20: 366-373.

Chen HW, Zheng J, Zhang X, Luo MB, Wang ZC, Qiao XL (2007). Surface desorption atmospheric pressure chemical ionization mass spectrometry for direct ambient sample analysis without toxic chemical contamination. J. Mass Spectrom., 42: 1045-1056.

Chiu YC, Yang HY, Lu SH, Chiang HK (2010). Micro-Raman spectroscopy identification of urinary stone composition from ureteroscopic lithotripsy urine powder. J. Raman Spectrosc., 41: 136-141.

Coe FL, Parks JH, Asplin JR (1996). The pathogenesis and treatment of kidney stones. N. Engl. J. Med., 327: 1141-1152.

Dai XH, Fang X, Zhang CM, Xu RF, Xu B (2007). Determination of serum uric acid using high-performance liquid chromatography (HPLC)/isotope dilution mass spectrometry (ID-MS) as a candidate reference method. J. Chromatogr., 857: 287-295.

De Souza PP, Augusti DV, Catharino RR, Siebald HGL, Eberlin MN, Augusti R(2007). Differentiation of rum and Brazilian artisan cachaca via electrospray ionization mass spectrometry fingerprinting. J. Mass Spectrom., 42: 1294-1299.

Evan AP, Coe FL, Lingeman JE, Worcester E (2005). Insights on the pathology of kidney stone formation. Urol. Res., 33: 383-389.

Ferrandino MN, Pierre SA, Simmons WN, Paulson EK, Albala DM, Preminger GM (2010). Dual-Energy computed tomography with advanced postimage acquisition data processing: improved determination of urinary stone composition. J. Endourol., 24: 47-354.

Herring LC (1962). Observations on the analysis of ten thousand urinary calculi. J. Urol., 88: 545-562.

Hiatt RA, Ettinger B, Caan B, Quesenberry CP, Duncan JD, Citron JT (1996). Randomized controlled trial of a low animal protein. High Fiber Diet in the Prevention of Recurrent Calcium Oxalate Kidney Stones, 144: 25-33.

Hu B, Peng XJ, Yang SP, Gu HW, Chen HW, Huan YF, Zhang TT, XL Qiao (2010). Fast quantitative detection of cocaine in beverages using nanoextractive electrospray ionization tandem mass spectrometry. J. Am. Soc. Mass Spectrom., 21: 290-293.

Jackson JE (1980). Principal components and factor-analysis.1. Principal components. J. Qual. Tech., 12: 201-213.

Jia LQ, Shen Y, Wang XM, He LJ, Xin Y, Hu YX (2009). Ultrasonographic diagnosis of urinary calculus caused by melamine in children. Chin. Med. J., 122: 252-256.

Johnson CM, Wilson DM, O'fallon WM, Malek RS (1979). Renal Stone Epidemiology: A 25-Year Study in Rochester. Minnesota. Kidney Int., 16: 624-631.

Lam CW, Lan L, Che XY, Tam S, Wong SY, Chen Y, Jin J, Tao SH, Tang XM, Yun KY, H PK (2009). Diagnosis and spectrum of melamine-related renal disease: Plausible mechanism of stone formation in humans. Clin. Chim. Acta., 402: 150-155.

Marickar YMF, Lekshmi P, Varma L, Koshy P (2009). EDAX versus FTIR in mixed stones. Urol. Res., 37: 271-276.

Mendonça JCF, Franca AS, Oliveira LS, Nunes M(2008). Chemical characterisation of non-defective and defective green arabica and robusta coffees by electrospray ionization-mass spectrometry (ESI-MS). Food Chem., 111: 490-497.

Millman S, Strauss AL, Parks JH, Coe FL (1982). Pathogenesis and clinical course of mixed calcium oxalate and uric acid nephrolithiasis. Kidney Int., 22: 366–370.

Moe OW (2006). Kidney stones: pathophysiology and medical management. The Lancet, 367: 333-344.

Moore BC (1981). Principal Component Analysis in Linear-Systems - controllability, observability and model-reduction. IEEE T. Automat. Contr., 26: 17-32.

Otnes B (1983). Urinary stone analysis methods, materials and value. Scand. J. Urol. Nephrol. Suppl., 71: 1–109.

Pietrow PK, Karellas ME (2006). Medical management of common urinary calculi. Am. Fam. Physician, 74: 86-94.

Sanvido GB, Garcia JS, Corilo YE, Vaz BG, Zacca JJ, Cosso RG, Eberlin MN, Peter MG (2010). Fast Screening and Secure Confirmation of Milk Powder Adulteration with Maltodextrin via Electrospray Ionization−Mass Spectrometry [ESI(+)−MS] and Selective Enzymatic Hydrolysis. J. Agric. Food Chem., 58: 9407-9412.

Sodhi RNS, Chen HW, Yang SP, Hu B, Zeng X, Xiao RH (2010). TOF-SIMS analysis of kidney stones possibly induced by the ingestion of melamine-containing milk products. Surf. Interface Anal., 43: 313-316.

Sun N, Shen Y, Sun Q, Li XR, Jia LQ, Zhang GJ, Zhang WP, Chen Z, Fan JF, Jiang YP, Feng DC, Zhang RF, Zhu XY, Xiao HZ (2009). Diagnosis and treatment of melamine-associated urinary calculus complicated with acute renal failure in infants and young children. Chin. Med. J., 122: 245-251.

Tipping ME, Bishop CM (1999). Probabilistic principal component analysis. J. R. Stat. Soc. B., 61: 611-622.

Wen JG, Yang HJ, Wang Y, Wang GX (2009). The clinical analysis of urolithiasis in 165 infants and children with history of feeding melamine contaminated milk powder. J. Urol., 5: S33.

Xin H, Stone R (2008). Tainted milk scandal Chinese probe unmasks high-tech adulteration with Melamine. Science, 322: 1310-1311.

Yang SP, Chen HW, Yang YL, Hu B, Zhang X, Zhou YF, Zang LL, Gu HW (2009). Imaging melamine in egg samples by surface desorption atmospheric pressure chemical ionization tandem mass spectrometry. Chin. J. Anal. Chem., 37: 315-318.

Yang SP, Ding JH, Zheng J, Hu B, Li JQ, Chen HW, Zhou ZQ, Qiao XL (2009). Detection of melamine in milk products by surface desorption

atmospheric pressure chemical ionization mass spectrometry. Anal. Chem., 81: 2426-2436.
Yang SP, Hu B, Li JQ, Han J, Zhang X, Chen HW, Liu Q, Liu QJ, Zheng J (2009). Surface desorption atmospheric pressure chemical ionization mass spectrometry for direct detection melamine in powdered milk products. Chin. J. Anal. Chem., 37: 691-694.
Zhang L, Wu LL, Wang YP, Liu AM, Zou CC, Zhao ZY (2009). Melamine-contaminated milk products induced urinary tract calculi in children. World J. Pediatr., 5: 31-35.
Zhu L, Gamez G, Chen HW, Chingin K, Zenobi R (2009). Rapid detection of melamine in untreated milk and wheat gluten by ultrasound-assisted extractive electrospray ionization mass spectrometry (EESI-MS). Chem. Commun., 5: 559-561.